13 February 1959, Volume 129, Number 3346

SCIENCE

CURRENT PROBLEMS IN RESEARCH

Shape of the Nucleus

It varies widely, from spherical for doubly magic nuclei to ellipsoidal and sometimes pear shapes.

Lawrence Wilets

Less than 50 years ago Lord Rutherford (1) laid the foundations for both the modern atomic and nuclear sciences with a series of celebrated experiments on the scattering of energetic alpha particles by thin foils. He used naturally radioactive materials as a source of the alpha projectiles and detected the scattered particles by visually observing flashes produced on a scintillation screen. From the pattern of light flashes, he was able to deduce that the (electrically neutral) atom consists of a positively charged, massive, nuclear core surrounded by a cloud of negatively charged electrons.

Earlier atomic theories fell; notable was J. J. Thompson's model of electrons embedded in a positively charged fluid. Two years later, in 1913, Niels Bohr (2) proposed his famous atomic model consisting of electrons circling the nucleus in quantized orbits.

Rutherford's experiments also yielded the first quantitative information on the size of the nucleus. The results indicated that the interaction between alpha particles and nuclei follows the Coulomb inverse square law for point charges down to distances of less than 10^{-11} centimeter. Later experiments by Rutherford and others revealed deviations from the Coulomb law, indicating structure at radii of the order of 10^{-12} centimeter.

During the past half century a diversity of experiments have been designed to measure the nuclear size and shape. These have included bombarding the nucleus with a variety of charged and neutral subatomic particles, probing the nuclear interior with its own atomic electrons, and observing nuclear radiations. Theoretical models have attempted to correlate less obvious nuclear properties, such as binding energy and reaction rates, with nuclear size.

The various experiments prior to 1953 were in qualitative agreement with respect to nuclear size, but did differ considerably when subjected to quantitative comparison. It was realized that at least part of the discrepancies could be attributed to insufficient knowledge of the nature of the probes, and another part to a lack of detailed theoretical understanding of nuclear structure.

Within the last 5 years there have been prodigious experimental advances in the detailed measurement of nuclear size, and theoreticians have been pressed to bring about a consistent interpretation of apparent disparities. The picture which is emerging is encouraging.

Within the same 5-year period exciting developments have occurred in the field of nuclear shape. Here, however, the theorists led the advances, opening up new areas of experimental research.

A picture of the gross structure—size and shape—of the nucleus can be presented now in a manner which would not have been possible 5 years ago. There is reason to believe that this picture will not be altered drastically in the next 5 years, although we look forward to a more comprehensive understanding of finer details of nuclear structure.

At this point discretion demands a few—but only a few—words concerning the use of pictures and models. While the nucleus can be described properly only in terms of actual experiments, the introduction of models can be expedient as an aid to the development of intuition and the stimulation of ingenuity. Concrete models generally contain more detail than can be verified experimentally, even in principle. Yet there can be no objection to the use of such idealized models if they are consistent with experiment and if their relationship to experiment is constantly borne in mind. Pictures, images, and models are used shamelessly in the present discourse.

This article is intended to present an "artist's conception" of the nucleus such as one might see through an out-of-focus and impossible-to-construct microscope. As the nucleus first enters the field of view of our hypothetical microscope, it appears as a formless mass. As we begin to adjust the focus, we are able to discern structure similar to that of a droplet of liquid, but with a diffuse surface. Some nuclei pulsate, passing from one shape to another. Others have permanently elongated shapes and rotate. As the focus improves, constituent parts appear. These are seen to be neutrons and protons (nucleons); occasionally there is a fleeting glimpse (10^{-23} second) of transient pi-mesons. But this is already further than we wish to proceed here, since we will not be concerned with the details of nuclear interiors.

General Nuclear Properties

The nucleus may be regarded as composed of neutrons and protons bound together by nuclear forces, the origin of which appears to lie in their mutual interaction with pi-mesons. It is far from trivial to comment that nucleons maintain their identity inside the nucleus, since one cannot easily describe other particles which are emitted by nuclei, such as electrons, neutrinos, and so forth, as existing *within* the nucleus.

The density of nuclear matter appears to be constant from one nucleus to another. To the extent that we can ascribe

Dr. Wilets, formerly of the Los Alamos Scientific Laboratory, Los Alamos, N.M., is now on the staff of the physics department, University of Washington, Seattle.

a boundary to the nucleus, this means that the nuclear volume is proportional to the nuclear mass number A. (The nuclear mass, proton, and neutron numbers are designated by the integers A, z, and N, respectively. $Z+N=A$.) For a spherical nucleus of volume $(4/3)\pi R^3$, the radius R can be written in the form

$$R = r_0 A^{1/3} \quad (1)$$

where r_0 is a constant.

Both experimentally and theoretically, it is convenient to divide the discussion of size and shape into two general categories, according to the nature of the probe.

The first category is the matter distribution, which corresponds to the distribution of neutrons and protons. What can be measured quite accurately is the distribution of charge, which, properly speaking, is not the same as the distribution of protons, since the proton itself has a measurable charge distribution. By examining the nuclear electrostatic field, the charge distribution can be deduced; the laws of electricity and magnetism are among the best understood in physics —at least within the realm of sizes under consideration.

The second category is the nuclear force field. The force field can be measured through its interaction with other nucleons, but the interpretation with respect to matter distribution depends upon a detailed nuclear model. It is customary, therefore, to present a description of the nuclear force field as such, and then challenge the theorist for an interpretation. The problem of the nuclear force field will not be discussed here except to comment that it is similar in shape to the matter distribution, but extends about 1.5×10^{-13} centimeter further (*3*).

Radial Distribution of Nuclear Matter

Electric probes. The electron and mu-meson are excellent probes for the nuclear electric field. Both may be considered to be structureless (*4*), point particles, and both interact with nuclear matter extremely weakly (the electron, immeasurably weakly) except through the electric field. The most accurate measurements of the nuclear charge distribution come from experiments with mu-mesic atoms and high energy electron scattering.

Mu-mesic atoms. A negative mu-meson impinging on an atom can be captured by the attractive electric field of the nucleus to form a structure similar to that of the hydrogen atom. It differs from hydrogen in that the nuclear charge, Z, may be 1 to 100 times greater and that the mu-meson is 207 times as heavy as an electron. The radii of the mesic orbits are inversely proportional to both the nuclear charge and the mesic mass. The inner orbits lie well inside the atomic electron orbits, thus preserving the one-particle, hydrogen-like character of the spectrum. In heavy elements, the lowest mesic orbit is quite comparable to the nuclear radius. The mu-meson is thus amply capable of exploring the electric field of the nucleus at close range. The experimental data come from the electromagnetic radiation (in the x- and gamma-ray regions) emitted when the meson jumps from one Bohr orbit to another.

The first observation of radiation from mesic atoms was reported in 1949 by Chang (*5*), who was working with cosmic ray mesons. A theoretical discussion

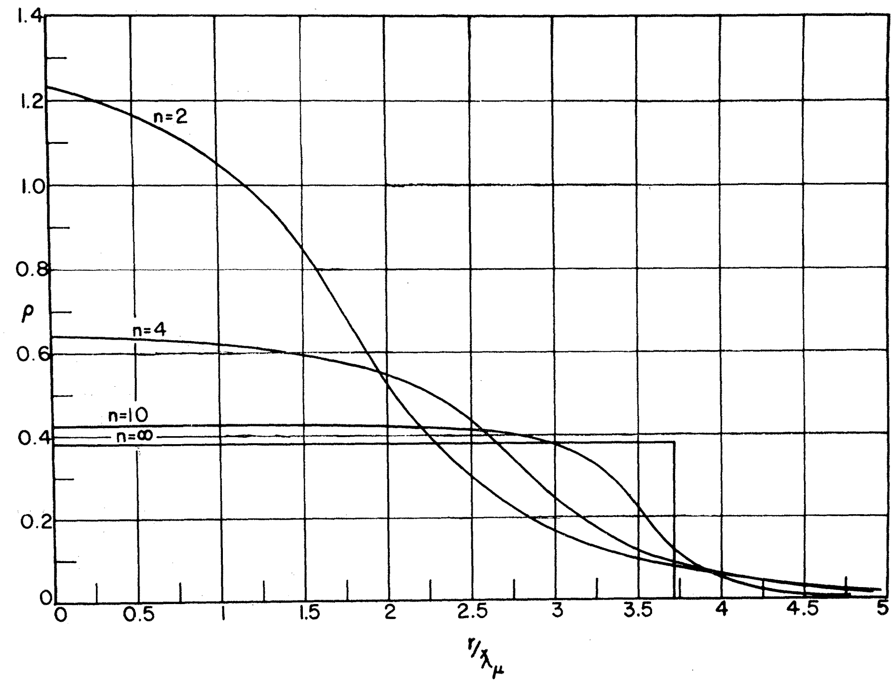

Fig. 1. A particular family of radial charge distributions, any one of which describes the mu-meson atomic radiation in lead. Each curve has only one adjustable parameter. Lengths are measured in units of the mu-meson reduced Compton wavelength, $ƛ_\mu = 2.1 \times 10^{-13}$ cm. [Reproduced from D. L. Hill and K. W. Ford, *Phys. Rev.* **94**, 1617 (1954)]

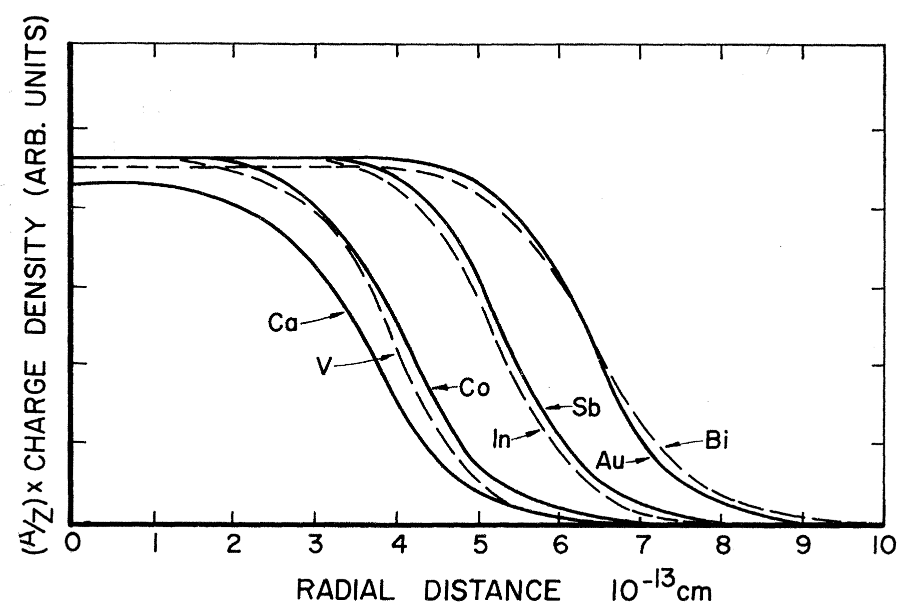

Fig. 2. Radial density (A/Z times charge) distribution curves for several elements. The curves are of the form given in Eq. 3, with two experimentally adjustable parameters, R and a. (Adapted from R. Hofstadter, *10*.)

by Wheeler (*6*) appeared the same year. With the advent of high-energy accelerators capable of producing copius numbers of mu-mesons, precision measurements on mesic atoms were begun, starting in 1953 with Fitch and Rainwater (*7*).

The present experiments have concentrated on the resonance line only, and yield a single parameter, which may be interpreted as the nuclear size (*8, 9*). There exist an infinity of different charge distributions consistent with the observed resonance line frequencies of the various elements. In Fig. 1 is shown a family of radial charge density distributions varying from exponential to uniform, all of which are compatible with experiment. Were the charge density uniform, the nuclear radius would be given by $1.17 \times 10^{13} A^{1/3}$ centimeter for lead. The accuracy of this number is about 1 percent, but these experiments do not yet give further information on the shape of the charge distribution.

Electron scattering. Employing the Stanford linear electron accelerator, Hofstadter and his co-workers (*10*) in 1953 began a program of electron-nuclear scattering which has contributed profoundly to our knowledge of the nuclear charge distribution. The amount of detail obtainable from the experiments is limited by the wave nature of electrons, which can only explore details of the order of, or larger than, their wavelength divided by 2π. The de Broglie relationship

$$\lambda = h/p \approx hc/E \qquad (2)$$

shows the value of using high-energy electrons (λ is the electron wavelength, h is Plank's constant, p is the electron momentum, E is the energy, and c is the velocity of light; for very energetic electrons, $E \approx cp$). At 180 Mev, the highest energy used by Hofstadter for all but the lightest nuclei, the characteristic length, $\lambda/2\pi$, is 10^{-13} centimeter. There is a limit as to how high an energy it is desirable to use, since eventually one would destroy the structure of the nucleus by the scattering process and essentially scatter independently from the individual nucleons. This would set in at wavelengths comparable to the internucleonic distance, r_0.

Analyses of the electron scattering experiments (*9–11*) are consistent with a charge distribution of rather uniform central density and a somewhat diffuse surface region. The central matter density (A/Z times the charge density) is quite constant from nucleus to nucleus. The analyses of the experiments do not rule out a central bump or depression of several percent, although neither is clearly indicated. At one time it was thought that the electrostatic repulsion between protons would tend to push charge to the nuclear surface. Because it is energetically unfavorable to separate neutrons and protons, and because nuclear matter appears to be quite incompressible (or inextensible), the theoretical indications are that a depression of more than a few percent is unlikely (*12*). At present, the electron scattering experiments are insensitive to further details in the charge distribution.

It is convenient to express the information available in terms of an explicit function for the density distribution. Reasonability criteria are applied in the selection of the expression: the function must be smooth and, from general quantum mechanical considerations, must fall off exponentially at large distances. A two-parameter function popularly chosen to express the density (in spherical symmetry) is given by

$$\rho(r) = \frac{\rho(0)}{1 + e^{(r-R)/a}} \qquad (3)$$

where $\rho(0)$ is the (approximate) central density, R is the half-density radius, and a is a surface thickness parameter.

The half-density radius for heavy nuclei follows an $A^{1/3}$ law of the form given in Eq. 1, with the empirical value of the constant given by

$$r_0 = 1.07 \times 10^{-13}\ \text{cm} \qquad (4)$$

This number can be measured to an accuracy of 1 percent for any given nucleus and fluctuates by about 2 percent from nucleus to nucleus. The value of r_0 is actually larger for lighter nuclei, since it is the central density which remains constant.

The surface thickness is frequently expressed in terms of the distance, D, in which the density falls from 90 to 10 percent of the central density. This quantity is related to the surface thickness parameter a (Eq. 3) by $D = 4.39a$. Analyses of the experiments yield (to an accuracy of about 10 percent)

$$D = 2.4 \times 10^{-13}\ \text{cm} \qquad (5)$$

independently of A. For a heavy nucleus, this is roughly one-third of the nuclear radius.

In Fig. 2 are shown experimentally ad-

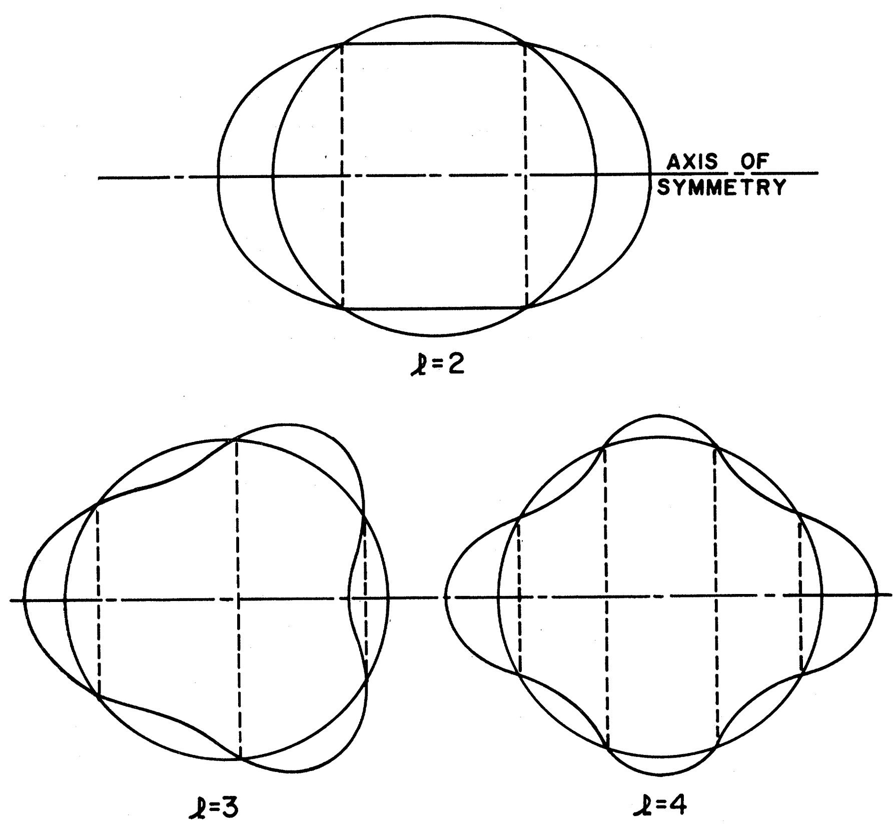

Fig. 3. Examples of the first few deformation modes. There are $(2l + 1)$ modes for a given order l, but only one of each order is shown, namely, the axially symmetric mode. The order $l = 0$ corresponds to a spherical shape (no deformation), while a small admixture of $l = 1$ corresponds to a translation of the body without deformation. The broken curves are nodal lines, the intersection of the surface with the undeformed sphere. The number of nodal lines equals the order l.

justed distribution functions of the form of Eq. 3 for several nuclei.

Structure of the proton. The lightest nucleus, the proton, has a complex structure. Although the theory of this structure is far from complete, the following picture is helpful in understanding what is going on. One begins with the concept of a *bare* nucleon (neutron or proton), a structureless particle which constantly emits and reabsorbs pi-mesons and, to a lesser extent, other particles. The *physical* nucleon consists of the bare nucleon plus its meson cloud. A particular emission and reabsorption process which contributes to the proton charge distribution is, conceptually, of the type

$$P \rightleftarrows N + \pi^+ \qquad (6)$$

where P and N represent the bare proton and neutron, and π^+ a positively charged pi-meson. While the system is in the state given by the left-hand side of Eq. 6, the charge may be considered concentrated at a point, but when the system is in the state specified by the right-hand side of Eq. 6, the charge is distributed over a reduced meson Compton wavelength, $h/2\pi m_\pi c = 1.4 \times 10^{-13}$ centimeter, where m_π is the mass of the pi-meson. Other processes, involving strange particles, nucleons-antinucleons, and so forth, can also contribute.

The Stanford electron scattering experiments (*3, 10*) have yielded structure in the proton. The data have been analyzed, assuming a charge distribution of the form

$$\rho_{\mathrm{prot}}(r) = e^{-r/b}/8\pi b^3 \qquad (7)$$

where the characteristic length b was found to have the value 0.23×10^{-13} centimeter.

The neutron appears to have very little charge distribution surrounding it. Even though the total net charge is zero, one can conceive of shell-like clouds of opposite charge at different radii; such have not been observed.

Distribution of protons in the nucleus. From the nuclear charge distribution and from the charge distribution of the proton, we can unfold the distribution of the *centers of the protons.* It is easier to consider first that the distribution of proton-centers, $\rho_0(\mathbf{r})$, is known. Then, given the proton charge distribution $\rho_{\mathrm{prot}}(r)$, the charge distribution is given by

$$\rho(\mathbf{r}) = \int \rho_{\mathrm{prot}}(|\mathbf{r} - \mathbf{r}'|)\rho_0(\mathbf{r}')\,d\tau' \qquad (8)$$

where $d\tau'$ is the volume element. Although this may be a complicated function in general, some simple features emerge directly. Consider the mean square radii, defined by

$$< r^2 > \, \equiv \int \rho(r) r^2 d\tau \qquad (9)$$

and similarly for the proton charge and proton-center distributions. The mean square radii for the three distributions are simply related by

$$< r^2 > \, = \, < r^2 >_0 + < r^2 >_{\mathrm{prot}} \qquad (10)$$

The charge distribution thus extends further than the proton-center distribution. For a large nucleus, the half-density radii of both distributions are nearly equal, but the surface thickness is greater for the charge distribution. The observed charge surface thickness, D, is related to that of the proton center distribution, D_0, by the relationship

$$D \approx D_0 + 4b^2/a \qquad (11)$$

with a defined in Eq. 3 and b in Eq. 7. The surface thickness for the proton-center distribution comes out to be $D_0 = 2.0 \times 10^{-13}$ centimeter.

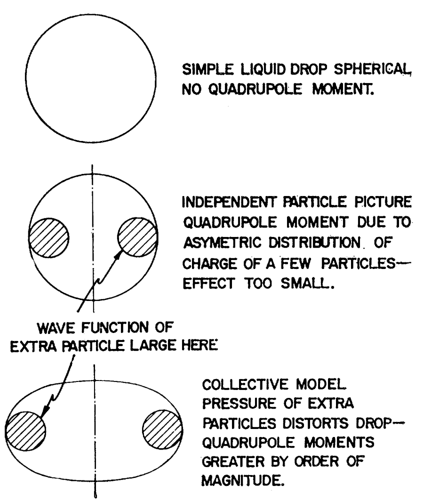

Fig. 4. An illustration of Rainwater's principle for an individual nucleon deforming a nuclear core. The shaded area represents the nucleon's wave function (orbit). Centrifugal force exerted by the nucleon deforms the core into an oblate spheroidal shape, as a marble orbiting rapidly inside a balloon would do. (Reproduced from D. L. Hill and J. A. Wheeler, *Phys. Rev.* **89**, 1106 [1953].)

There is little more one can say, from the experimental data, to pin down a proton matter—or mass—distribution. There is certainly mass associated with the charged cloud surrounding the proton. The pi-mesons (which probably predominate in the cloud) are lighter by a factor of nearly seven, which would tend to indicate that most of the mass is concentrated at the proton-center. But there are unresolved theoretical problems which prevent us from pursuing the problem further at this date: for example, the *nature* of the nucleonic mass is not properly understood.

Distribution of neutrons. There exist no experiments capable of yielding so "clean" a description of the neutron distribution as exist for protons. However, it is possible to obtain a measure of the difference between neutron and proton distributions. For example, at certain energies, negative pi-mesons interact more strongly with protons than do positive pi-mesons; at the same energy, the reverse is true for meson-neutron interaction. Loosely speaking, scattering with negative pis measures a proton distribution, and scattering with positive pis, a neutron distribution. Because of the nature of the pi-meson as a probe, the proton distribution so obtained will not be the same as either the charge or proton-center distributions. However, since the meson probe probably acts similarly for both neutrons and protons, the difference between (say) their half-distance radii is measured by the experiments. The best experiments to date show very little difference between the distributions (*13*):

$$R_P - R_N = (0.3 \pm 0.3) \times 10^{-13}\ \mathrm{cm} \qquad (12)$$

The smallness of this difference is contrary to earlier nuclear models which would put the protons in a spherical shell outside the neutrons—held out by their electrostatic repulsion. The explanation appears to be in a combination of factors (*12*): (i) the electric forces are weaker than nuclear forces; (ii) it is energetically favorable, because of the Pauli exclusion principle, for neutrons and protons to overlap as much as possible; and (iii) the electrostatic force under certain circumstances can act as a retaining wall to confine the protons, rather than as a dispersing influence.

Deformed Nuclei

A great deal of evidence has recently accumulated indicating that many nuclei possess shapes which differ considerably from spherical symmetry. The role of deformations in nuclear theory has been propounded by the protagonists of the so-called "collective" and "unified" models. The names associated with the theories include N. Bohr, J. Rainwater, A. Bohr, B. Mottelson, J. A. Wheeler, and others. The extent to which theory successfully charted the course of advance in this field of nuclear research is remarkable. It is a tribute to the dynamism of A. Bohr and Mottelson and the Copenhagen school of the unified model.

In the spirit of the historical development, the present discussion begins with a description of the models, and later deals with some experimental verification. Consistent with the previous discussion of density distributions, we are still concerned here with only gross (collective) features of nuclear shape, and generally avoid discussion of internal structure.

The collective model (*14*). For the discussion of certain properties, the nucleus may be regarded as a uniformly charged, incompressible, viscosity-free, liquid drop. The dynamics of the drop are governed by the assumption of irrotational fluid flow (no vortices). It is usually assumed that a well-defined surface exists; in the case of a diffuse edge, the surface may be specifically defined as the locus of half-density points.

The only forces, (or potential energies) involved in this model are electrostatic force and surface tension (surface energy $= S \times$ area of the surface, where S is a constant. The electrostatic force tends to deform or rupture the droplet, while the surface tension tends to contain the droplet and maintain sphericity.

This is certainly a simple model. Yet with the elementary assumptions stated above, N. Bohr and J. A. Wheeler (*15*) in 1939 were able to arrive at a qualitative understanding of nuclear fission. The single parameter characterizing a nucleus for fissionability (in this model) is the ratio, x, of electrostatic to twice surface energy:

$$x = E_{es}/2E_S = \frac{3}{5}\,\frac{Z^2e^2}{R}/2S\,4\pi R^2 = \frac{Z^2}{A}\Big/\left(\frac{Z^2}{A}\right)_c \qquad (13)$$

The constant $(Z^2/A)_c$ has a numerical value of 47.8. If x is greater than unity, the spherical shape is energetically unstable and fission will proceed spontaneously. But for x less than unity, the spherical shape is at least locally stable, although certain critical, deformed shapes exist beyond which further deformation, and eventually fission, is energetically favored. It requires energy of excitation to bring the droplet to these critical shapes.

For $x < 1$, and with less energy of excitation available than is required for fission, the droplet executes volume-preserving, oscillatory motion which has the nature of surface waves. If the amplitudes of oscillation are small, a normal mode analysis can be made. The modes can be classified according to the number (order l) of oscillations on the surface (see Fig. 3). (The classification can be made more precise by introducing nodal lines, defined as the intersection of the surface with the equilibrium sphere. Then the order is the number of nodal lines.) There are $(2l+1)$ independent normal modes of a given order l. The quantum mechanical energy level spectrum of the droplet is that of a set of uncoupled, harmonic oscillators.

It does not make much sense, from the viewpoint of a collective description, to include orders where the wavelength divided by 2π is comparable to, or smaller than, the mean internucleonic distance r_0. The mean wavelength is of the order of $2\pi R/l = 2\pi\, r_0 A^{1/3}/l$. This restricts l to values less than $A^{1/3}$.

The unified model (*14, 16*). A model which appears quite different from the collective model but which also had considerable success is the independent particle, or shell, model. In this model the nucleons move about freely within the nuclear interior, interacting only weakly with one another but experiencing a common nuclear potential. The unified model obtains its name from attempts to bring about a consistent interpretation of the collective and independent particle models. It was first suggested by Rainwater that individual nucleons may affect the collective behavior of the droplet. One of the most dramatic manifestations of the collective-individual nucleon interplay is the occurrence of large, permanent deformations. This is illustrated in Fig. 4. We begin with a spherical droplet, sometimes called a core. An additional nucleon moves freely within the core, the droplet surface acting to confine the nucleon. The nucleon, moving in a circular orbit as shown, exerts a centrifugal force on the droplet surface, tending to deform it into an oblate (pancake-shaped) spheroid. (A spheroid is an ellipsoid with two axes equal.) A second nucleon can fill a similar, but oppositely rotating, orbit. This will tend to double the magnitude of the deformation. But, according to the Pauli exclusion principle, only one nucleon can occupy a given orbit, and so subsequent nucleons will occupy orbits oriented less favorably to increase deformation.

Now, the nucleonic magic numbers (2, 8, 20, 28, 50, 82, 126) represent highly stable configurations for either neutrons or protons, similar to the electronic configurations in the noble gases.

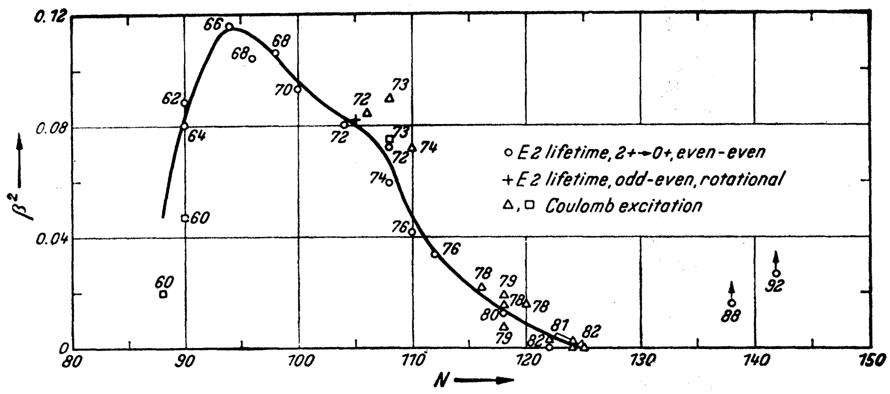

Fig. 6. The square of nuclear deformation plotted as a function of N in the first rare earth period ($\varepsilon^2 = (45/16\pi)\beta^2 = 0.895\beta^2$). Neutron magic numbers occur at 82 and 126. The proton number, Z, is given near each point. (Reproduced from K. W. Ford and D. L. Hill, *9*.)

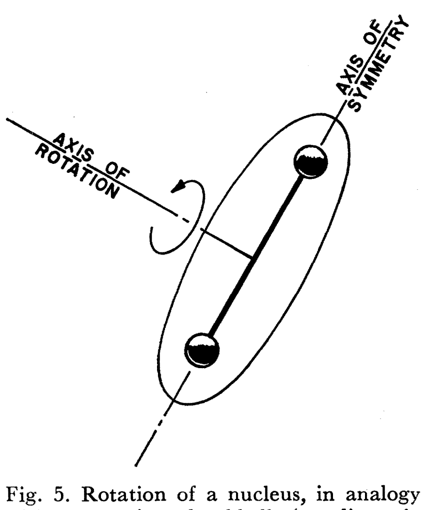

Fig. 5. Rotation of a nucleus, in analogy with a rotating dumbbell (or diatomic molecule). Because the moment of inertia is very small along the axis of symmetry, the object rotates about an axis perpendicular to the symmetry axis. The example is for an even-Z, even-N nucleus, where there is no internal angular momentum to be considered.

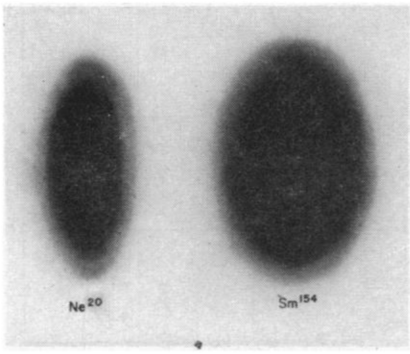

Fig. 7. Scaled "sketches" of the most deformed nucleus in the light and in the medium weight regions. Ne^{20} may have an ε as great as 0.85 (*19*), while Sm^{154} has $\varepsilon \sim 0.35$.

They are assumed to prefer spherical symmetry; when both neutron and proton configurations are magic, they form the "core" referred to in the previous paragraph. When sufficient nucleons have been added to a core to arrive at the next higher doubly magic number, the nuclear equilibrium shape returns to spherical. It is interesting to note that one particle less than a magic number (sometimes referred to as a hole) exerts a negative pressure on the surface, leading to a prolate (cigar-shaped) spheroid. Midway between magic numbers, the simple theory predicts a switch from oblate to prolate. Details in the nuclear force, however, lead to a predominance of prolate shapes. We shall refer below primarily to prolate shapes, although nearly everything is equally valid for the oblate case.

It is clear that the magnitude of nuclear deformations depends on the details of the internal structure of the nucleus, and may be expected to vary considerably, from nucleus to nucleus. The variation has some regularity, nevertheless, the deformations reaching a maximum between magic configurations.

In addition to being able to vibrate about the deformed equilibrium shape, the spheroidal droplet can also rotate. In fact, it is energetically easier (in the sense that the quantum mechanical energy levels lie lower) for the spheroid to rotate than to vibrate.

If we look for a macroscopic analog of our cigar-shaped nucleus, we should not look to a rigid body of this shape. An egg might be better, so long as it is not hard-boiled (*17*). The point is this: of the three moments of inertia for a rotating nucleus, the moment for rotations about the symmetry axis (axis of revolution) vanishes. A body nearly having such a property is a dumbbell (or diatomic molecule) in which the weights lie very close to the rod (see Fig. 5). No matter how an *idealized* dumbbell is thrown into the air, it always rotates end over end, about an axis perpendicular to to the rod.

The smallness of the moment of inertia about the symmetry axis is an interesting and important point. It has been given considerable theoretical attention, along with the entire nuclear moment of inertia problem. In spite of sophisticated progress, an early naïve analogy still serves as the best aid to understanding. Consider a bucket of water which is maintained upright and spun about its vertical, central axis. If there were no viscosity between the bucket and the water, the water would not be set in motion and hence would offer no inertial resistance to the rotation. Consider next the bucket to be bent so that from above it looks like an ellipse; rotation about the same axis now necessitates moving water. As the deformation of the bucket is increased, the moment of inertia associated with the water increases. The rotation of the circular bucket corresponds to droplet rotations about the symmetry axis, while rotation of the distorted, elliptical bucket corresponds to droplet rotation about an axis perpendicular to the symmetry axis.

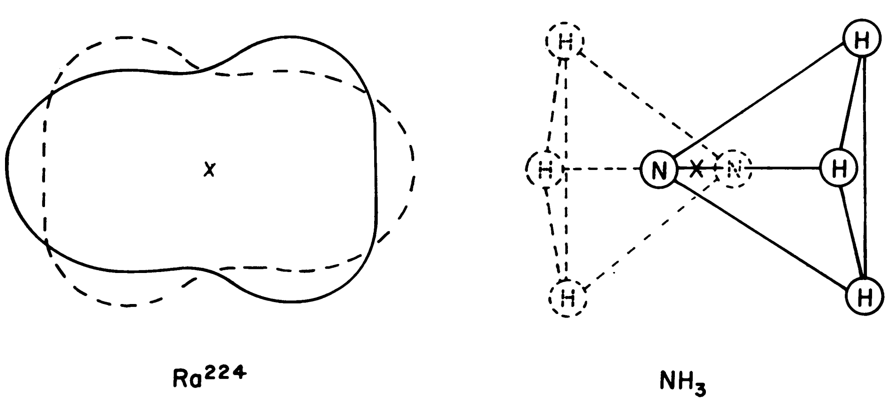

Fig. 8. Schematic representation of a pear-shaped nucleus, compared with an equally schematic representation of the ammonia molecule, NH_3. The broken curves indicate the inverted configurations. The crosses are the centers of mass.

Consequences of nuclear deformations (*16*). One rather direct manifestation of nuclear deformations is the deviation of the nuclear electric field from spherical symmetry. A quantity of interest is the nuclear quadrupole moment, defined by

$$Q = \int \rho(\mathbf{r})(3z^2 - r^2)d\tau \qquad (14)$$

where $\rho(\mathbf{r})$ is the nuclear electric charge density and $d\tau$ is the elemental volume. (Note that Q vanishes if $\rho(\mathbf{r})$ is spherically symmetric.)

Static quadrupole moments can be measured by atomic spectroscopy and molecular resonance techniques. Furthermore, a rotating or oscillating quadrupole can radiate or absorb electromagnetic energy. The rate of emission (lifetime) or probability for absorption (cross section) of radiation gives a measure of the *transition* quadrupole moment. Although these two moments are operationally different quantities, the model provides a relationship between them in terms of an *intrinsic* quadrupole moment. For a uniformly charged spheroid, the intrinsic quadrupole moment, Q_0 (defined as in Eq. 14, with z taken along the nuclear symmetry axis), is related to the deformation by

$$Q_0 \cong \frac{4}{5} ZR^2\varepsilon \qquad (15)$$

where R is the mean nuclear radius, and the deformation parameter, ε, is defined here as the difference between the length of the spheroid along the symmetry axis and the width perpendicular to the symmetry axis, divided by twice the mean radius (*18*). Positive values of ε correspond to prolate, and negative to oblate, spheroids.

Other experimental verifications of the unified model come from the occurrence of rotational energy level spectra, new selection rules on alpha, beta, and gamma transitions, nuclear spins and parities, details of level structure, magnetic moments, and a variety of other experiments.

Occurrence of nuclear deformations. Large permanent deformations of the type discussed above occur with great regularity in three regions of the nuclear masses. These are $19 < A < 25$, $150 < A < 185$, and $220 < A$. (Note that doubly magic nuclei appear at $A = 8 + 8 = 16$, $50 + 82 = 132$, and $82 + 126 = 208$.) The lightest region was the most recently recognized (*19*), coming as a bit of surprise, since collective concepts were not expected to be valid for so few nucleons. The other two regions correspond coincidently to the chemical rare earth regions. Large deformations actually appear very abruptly at $N = 90$ (near A of 150) and depend more strongly on N than on Z in the first rare earth region. Similarly, large deformations begin again at $Z = 88$ (near A of 220) and depend more strongly on Z in the second rare earth region. All nuclei so far observed in the limits of these last two regions display unified model characteristics.

In Fig. 6 is shown a plot of experimentally determined deformations in the first rare earth region. Note the sharp rise at 90 neutrons, and the smallness of the deformations at the doubly magic numbers. In Fig. 7 are scaled drawings of the most deformed nuclei in the light and intermediate mass regions, namely, Ne^{20} and Sm^{154}.

Pear-shaped nuclei. The final type of deformation to be discussed is the "pear-shape." This is a deformation involving a combination of both $l=2$ and $l=3$ modes (see Fig. 8).

Speculation that such pear-shapes exist was first presented by Christy (*20*), and is based on details of the rotational-vibrational energy level spectrum. Certain isotopes in the neighborhood of radium exhibit a characteristic spectrum analogous to the so-called inversion spectrum of the ammonia molecule, NH_3. Both spectra have been interpreted as corresponding to oscillations of the objects between one relatively stable form to its mirror image, which is equally stable. This is illustrated in Fig. 8; the "mirror" passes through the center of masses of the objects and is oriented normal to the axes of symmetry.

The asymmetrical shape of such nuclei may also have relevance to the problem of mass asymmetry in fission. Most nuclei fission into fragments of quite unequal masses, which indicates that at some point before splitting actually occurs, fissioning nuclei prefer an asymmetrical shape.

Summary

The gross features of nuclear morphology can be summarized as follows. Nuclei have shapes similar to a diffuse-surfaced, liquid drop. The interior density is rather uniform, and also constant from nucleus to nucleus. The constancy of nuclear density implies an $A^{1/3}$ law for the mean nuclear radius, the proportionality constant being 1.07×10^{-13} centimeter. The surface region is diffuse, the nuclear density falling from 90 to 10 percent of the central value in a distance of about 2.4×10^{-13} centimeter, independently of nuclear mass number.

Nuclear shapes can vary rather widely, with doubly magic nuclei preferring spherical symmetry. Some nuclei execute volume-preserving oscillations about spherical shape, while others possess permanent spheroidal deformations. The values of the deformation parameter, ε, for such spheroids possibly attains 0.85 for some light nuclei and 0.4 for some intermediate weight nuclei.

There is some evidence, based on the occurrence of "inversion" spectra and asymmetrical fission, that pear-shaped nuclei may also exist.

References and Notes

1. E. Rutherford, *Phil. Mag.* 21, 669 (1911).
2. N. Bohr, *ibid.* 26, 476 (1913).
3. A collection of review articles based on the Stanford Conference on Nuclear Size appears in *Revs. Mod. Phys.* 30 (April 1958).
4. Both particles possess intrinsic spin ($h/4\pi$) and intrinsic magnetic moment ($eh/4\pi mc$), but these two characteristics are exhibited by the Dirac equation for point particles, which the electron and mu-meson appear to obey very accurately.
5. W. Y. Chang, *Revs. Mod. Phys.* 21, 166 (1949); *Phys. Rev.* 75, 1315 (1949).
6. J. A. Wheeler, *Revs. Mod. Phys.* 21, 133 (1949).
7. V. L. Fitch and J. Rainwater, *Phys. Rev.* 92, 789 (1953).
8. L. N. Cooper and E. M. Henley, *ibid.* 92, 801 (1953).
9. K. W. Ford and D. L. Hill, *Ann. Rev. Nuclear Sci.* 5, 25 (1955); D. L. Hill, *Encyclopedia of Physics* (Springer, Heidelberg, 1957), vol. 39, p. 178.
10. A review of electron scattering experiments and analyses by R. Hofstadter appears in *Revs. Mod. Phys.* 28, 214 (1956).
11. D. G. Ravenhall and D. R. Yennie, *Phys. Rev.* 96, 239 (1954).
12. L. Wilets, *ibid.* 101, 1805 (1956); *Revs. Mod. Phys.* 30, 542 (1958).
13. A. Abashian, R. Cool, J. R. Cronin, *Phys. Rev.* 104, 855 (1956); see also W. N. Hess and B. J. Moyer, *ibid.* 101, 337 (1956), and R. W. Williams, *ibid.* 98, 1387 (1955).
14. A. Bohr, *Kgl. Danske Videnskab. Selskab. Mat.-fys. Medd.* 26, No. 14 (1952).
15. N. Bohr and J. A. Wheeler, *Phys. Rev.* 56, 426 (1939).
16. J. Rainwater, *Phys. Rev.* 79, 432 (1950); A. Bohr and B. R. Mottelson, *Kgl. Danske Videnskab. Selskab. Mat.-fys. Medd.* 27, No. 16 (1953). A general review is given by S. Moszkowski in *Encyclopedia of Physics* (Springer, Heidelberg, 1957), vol. 39, p. 411.
17. A hard-boiled egg is essentially a solid body with three nonvanishing moments of inertia. A raw egg nearly satisfies the idealized bucket experiment of the next paragraph of this article. Rotation of the egg shell about its symmetry axis is decoupled from the egg fluid so there is very little moment of inertia about this axis. One can easily verify the difficulty of spinning a raw egg about its symmetry axis. If one gives a spin and lets go, the egg usually ends up spinning about an axis normal to the symmetry axis.
18. The deformation parameter ε defined here is related to Bohr's β (*14*) by $\varepsilon = (45/16\pi)^{1/2}\beta = 0.946\beta$.
19. See, for example, G. Rakavy, *Nuclear Phys.* 4, 375 (1957).
20. R. Christy (unpublished); see also F. S. Stevens, F. Asaro, I. Perlman, *Phys. Rev.* 100, 1543 (1955); K. Lee and D. R. Inglis, *ibid.* 108, 774 (1957).